

Extensive decentralized hydrogen export from the Atlantis Massif

Susan Q. Lang^{1*}, Marvin D. Lilley², Tamara Baumberger³, Gretchen L. Früh-Green⁴, Sharon L. Walker⁵, William J. Brazelton⁶, Deborah S. Kelley², Mitchell Elend², David A. Butterfield⁷ and Aaron J. Mau¹

¹School of the Earth, Ocean, and Environment, University of South Carolina, Columbia, South Carolina 29208, USA

²School of Oceanography, University of Washington, Seattle, Washington 98105, USA

³Cooperative Institute of Marine Resources Studies, Oregon State University, and Pacific Marine Environmental Laboratory (PMEL), National Oceanic and Atmospheric Administration (NOAA), Newport, Oregon 97365, USA

⁴Department of Earth Sciences, ETH Zürich, 8092 Zurich, Switzerland

⁵PMEL, Office of Oceanic and Atmospheric Research (OAR), NOAA, Seattle, Washington 98115, USA

⁶School of Biological Sciences, University of Utah, Salt Lake City, Utah 84132, USA

⁷University of Washington/Joint Institute for the Study of the Atmosphere and Ocean (JISAO) and PMEL, NOAA, Seattle, Washington 98115, USA

ABSTRACT

Hydrogen is an important energy source for subsurface microbial communities, but its availability beyond the flow focused through hydrothermal chimneys is largely unknown. We report the widespread export of H₂ across the Atlantis Massif oceanic core complex (30°N, Mid-Atlantic Ridge; up to 44 nM), which is distinct from the circulation system feeding the Lost City Hydrothermal Field (LCHF) on the massif's southern wall. Methane (CH₄) abundances are generally low to undetectable (<3 nM) in fluids that are not derived from the LCHF. Reducing fluids exit the seafloor over a wide geographical area and depth range, including the summit of the massif and along steep areas of mass wasting east of the field. The depth of the fluids in the water column and their H₂/CH₄ ratios indicate that some are sourced separately from the LCHF. We argue that extensive H₂ export is the natural consequence of fluid flow pathways strongly influenced by tectonic features and the volume and density changes that occur when ultramafic rocks react to form serpentinites, producing H₂ as a by-product. Furthermore, the circulation of H₂-rich fluids through uplifted mantle rocks at moderate temperatures provides geographically expansive and stable environmental conditions for the early evolution of biochemical pathways. These results provide insight into the spatial extent of H₂- and CH₄-bearing fluids associated with serpentinitization, independent of the focused flow emanating from the LCHF.

INTRODUCTION

A continuous supply of hydrogen formed by the interaction of water with mantle rocks may have driven the formation of organic molecules on early Earth and other planets, laying the prebiotic groundwork for life (Martin and Russell, 2007; Sojo et al., 2016). Hydrogen likely fueled the development and evolution of early life, as several lines of evidence point to a central role of H₂-utilizing metabolic pathways

in the last universal common ancestor (Weiss et al., 2017).

Fuel alone is not sufficient for the formation of prebiotic organics and early life. Conductive temperatures, availability of inorganic carbon, mineral surfaces, wet-dry cycles, and metal catalysts also determine reaction extents and shape the earliest biomolecules necessary to harness energy and transfer information (e.g., Yu et al., 2013; Camprubi et al., 2017; Frenkel-Pinter et al., 2020). In this context, the locations and environmental conditions in which

H₂ forms are as important as the quantities that are generated.

We report the widespread export of H₂ across the Atlantis Massif oceanic core complex (Mid-Atlantic Ridge, 30°N), which is distinct from the circulation system and channeled flow of the nearby Lost City Hydrothermal Field (LCHF). This type of decentralized export starkly contrasts with magmatic-dominated systems at mid-ocean ridges where hot, buoyant fluids discharging from depths of ~1–3 km are channeled into high-permeability up-flow zones (Fisher, 2004; McCaig et al., 2007). The Atlantis Massif decentralized fluids are elevated in H₂ and migrate through environments that satisfy multiple requirements for the development of early life.

METHODS

Samples and data were collected during International Ocean Discovery Program (IODP) Expedition 357 (October 2015) and the Lost City 2018 Return expedition (September 2018) (see Text S1 in the Supplemental Material¹). In both expeditions, water column samples collected by hydrocasts were analyzed aboard the ship for volatile concentrations (H₂, CH₄) (Fig. 1; Figs. S1 and S2). In 2018, the remotely operated vehicle (ROV) *Jason* carried out visual seafloor surveys and was outfitted with *in situ* sensors that continually monitored oxidation-reduction potential (ORP) and temperature.

*E-mail: slang@geol.sc.edu

¹Supplemental Material. Detailed methods and supplemental figures. Please visit <https://doi.org/10.1130/G48322.1> to access the supplemental material, and contact editing@geosociety.org with any questions.

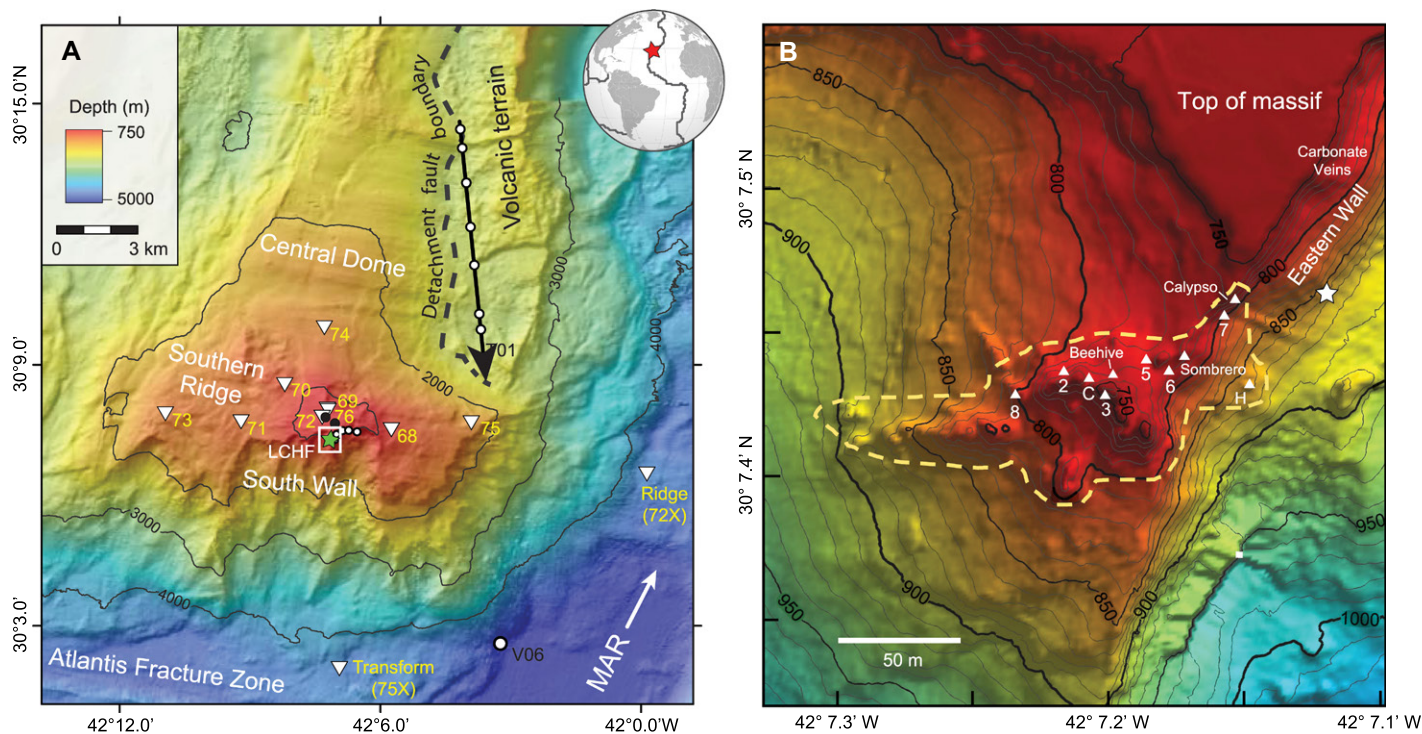


Figure 1. Bathymetric maps of (A) Atlantis Massif and (B) Lost City Hydrothermal Field (LCHF). International Ocean Discovery Program (IODP) Expedition 357 boreholes are denoted with yellow triangles, and 2018 hydrocasts are denoted by white circles. Niskin tow followed the black arrow, with white circles indicating individual bottle sample locations. Orifices shown in Figure 2 are denoted by black dots. LCHF is represented by the green star, and white box represents the area in panel B. MAR—Mid-Atlantic Ridge. In B, dashed yellow line shows extent of carbonate chimneys. Currently active structures are shown with white triangles. White star marks location of the photo mosaic in Figure S4 (see footnote 1). Depth contours are in meters.

RESULTS

Fluid Flow Across the Top of the Massif

The results from Expedition 357 were previously reported by Früh-Green et al. (2017, 2018) and are summarized here. Near-seabed hydrocasts across the top of the massif captured fluids with H_2 concentrations regularly in the tens of nanomolars and with a high of 44 nM above one of the central boreholes, compared to background seawater concentrations of <1 nM (Fig. 1; Table S2). Fluids flushed from the boreholes during drilling reached H_2 concentrations up to 322 nM (Table S1). In contrast, CH_4 concentrations were low to undetectable, ranging from below the detection limit of 0.3 nM to a high of 5 nM in hydrocast and borehole fluids (Tables S1 and S2).

In 2018, we also directly observed fluid flow at multiple locations across the top of the massif. Series of orthogonal veins along a sediment-free region at the top of the massif are infilled with carbonate (Fig. 1; Fig. S3). Similar fractures have been attributed to volume expansion during serpentinization (Denny et al., 2016). Active flow was confirmed by a 1 °C increase above background on a temperature probe.

Flow through the carbonate sands that cover much of the rocky surface over the central portion of the massif was also observed ~450 m and ~700 m north of LCHF (Fig. 1). Two orifices surrounded by bright white deposits were

identified while transiting (Fig. 2). When the ROV passed over the orifices, the ORP sensor dropped by 4.3–8.3 mV in conjunction with a 0.09–0.33 °C temperature increase, indicating active flow of a fluid more reducing than seawater.

Fluids Emanating from the Eastern Wall and the Termination of the Detachment Fault

Extensive fluid flow was also observed along the eastern wall of the Atlantis Massif (Fig. 1; Figs. S4 and S5). The cliff face is the surface of a steep normal fault that cuts gabbroic and ultramafic rocks within the detachment fault zone (Kelley et al., 2005; Karson et al., 2006).

Extensive carbonate deposits on the cliff face extend >200 m laterally at a depth of 800–850 m (Kelley et al., 2005). Large, actively venting, carbonate structures also rise from the cliff face and fall along the east-west major lineament on which most chimneys occur across the LCHF (Fig. 1B) (Kelley et al., 2005). In 2018, we identified a previously undocumented, nearly continuous series of carbonate deposits at depths of 855–870 m and extending laterally over 30 m (Fig. 1; Figs. S4 and S5). Fluids vented directly from the wall with geochemical characteristics ($T = 22$ °C; $pH_{22C} = 9.1$; $Mg = 36.6$ mM) similar to LCHF fluids.

We carried out hydrocasts along the eastern wall to cover a broader geographical area. The

casts captured fluids with elevated H_2 and CH_4 (18.7–40.8 nM and 5.4–10.6 nM, respectively) at 880–904 m depth, deeper than either identified contour of carbonate deposits or any known vents (Table S2; Figs. S6 and S7). Elevated H_2 concentrations (11.2–19.4 nM) were also detected extensively over the detachment fault termination boundary northeast of the LCHF (Fig. 1; Table S2).

DISCUSSION

Source of H_2 Distinct from the LCHF

The hydrocasts and seafloor surveys demonstrate that reducing fluids with elevated H_2 concentrations exit the seafloor over a wide geographical area and depth range. Because H_2 has a residence time of ~ 10 h in the water column (Kadko et al., 1990), its flux must be sufficient to continually resupply near-bottom waters. Three potential sources of this H_2 are: (1) entrainment of LCHF fluids with millimolar H_2 concentrations dispersed into a water column plume; (2) subsurface migration of LCHF vent fluids to distal exit points; or (3) localized sources distinct from LCHF circulation pathways.

The H_2/CH_4 ratios of the fluids can distinguish among these possibilities. LCHF fluids have H_2/CH_4 ratios of 0.9–9.2, with the highest values occurring in the hottest fluids (Proskurowski et al., 2006, 2008) (Fig. 3; Figs. S8 and S9). Subsurface microbial processes lower

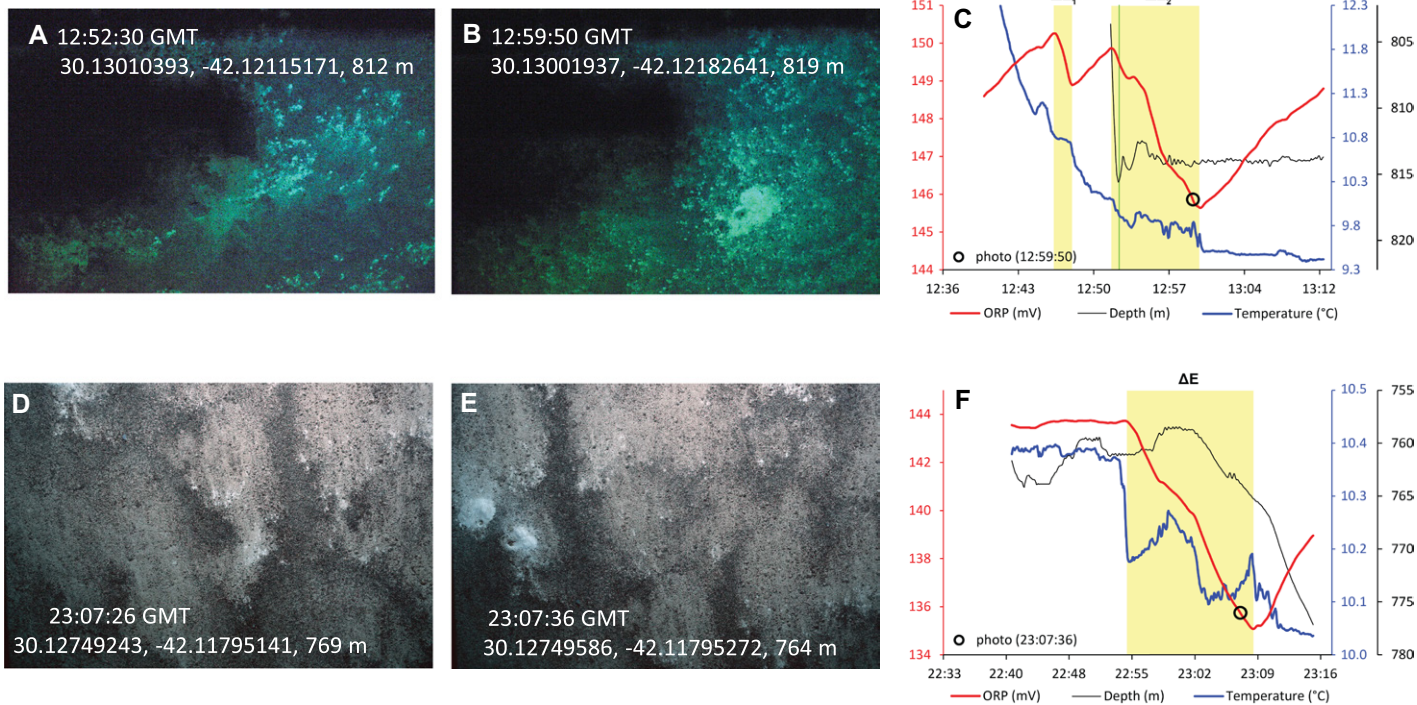


Figure 2. (A–F) Visual and sensor evidence of reduced fluids at the top of the Atlantis Massif collected during two remotely operated vehicle Jason transects. Images captured when vehicle was 4.2–4.5 m above the seabed depict typical sediments (A, D), in contrast to orifices surrounded by bright white sediments (B, E). Graphs show oxidation reduction potential (ORP) signal versus time in GMT (red line) and temperature versus time (blue line). Depth (black line) is shown when vehicle was <5 m above seafloor; changes are due to topography. (C) Graph depicts two substantial drops in ORP (ΔE); drops >0.5 mV are diagnostic of reducing hydrothermal effluent (Text S1 [see footnote 1]). $\Delta E_1 = -1.4$ mV (from 12:46–12:48:16 h) corresponds to descent of vehicle through Lost City Hydrothermal Field (LCHF) plume from ~750 to 775 m. $\Delta E_2 = -4.3$ mV occurred while transiting and corresponds with 0.18–0.33 °C temperature increase. (F) Graph depicts $\Delta E = -8.6$ mV from 11:54:36 to 23:09:11 h, with corresponding temperature spike of 0.09–0.13 °C.

this ratio through the consumption of H_2 and production of minor amounts of CH_4 (Lang et al., 2012; Proskurowski et al., 2006). Similar loss of H_2 and gain of CH_4 due to seafloor microbial activity occur in a myriad of other hydrothermal systems (Von Damm and Lilley, 2004; Wankel et al., 2011). Export into the water column dilutes the fluids, with no impact on this ratio, and promotes the oxidation of both volatiles by microorganisms. Because H_2 is consumed 10× more rapidly than CH_4 in the oxic water column (Kadko et al., 1990), fluids exported from the LCHF have H_2/CH_4 ratios lower than 9.2 (Larson et al., 2015). Therefore, fluids with H_2/CH_4 ratios higher than LCHF fluids (>9.2) cannot be attributed to export from the plume or subsurface migration.

The fluids seeping from the eastern wall have H_2/CH_4 ratios similar to or lower than those of the LCHF (Fig. 3; Figs. S8 and S9) and are likely an extension of the circulation pathway supplying the field. The fluids collected over the detachment fault boundary have H_2/CH_4 ratios (7.0–9.2) indistinguishable from LCHF fluids. However, it is unlikely that they are sourced from the main circulation pathway of LCHF because they egress 7–11 km to the northeast.

The majority of fluids exiting across the top of the massif have H_2/CH_4 ratios greater than those from LCHF (>9.2), pointing to an inde-

pendent source (Fig. 3; Figs. S8 and S9; Table S2). Most samples were collected deeper than 900 m, precluding input from the LCHF plume (Fig. 3; Table S2). The exception is the near-seabed fluids captured at the summit of the massif, at depths similar to LCHF chimneys (818 and 848 m; Früh-Green et al., 2017). The LCHF plume could have impacted these fluids, but the high H_2/CH_4 ratios (10–148) and evidence of fluid flow from nearby orifices are more consistent with largely local sources.

Geological Settings of H_2 -Rich Fluids Dispersed Across the Top of the Massif

The most likely source of H_2 across the top of the Atlantis Massif is ongoing, widespread serpentinization (Fig. 4). Geophysical modeling suggests that in addition to vent fluids channeled along relatively narrow flow paths, slower-moving fluids circulate in “low-flux backwaters of the system” (Titarenko and McCaig, 2016, p. 325). These backwater fluids would not reach the elevated temperatures of those in the LCHF, which are heated to 150–250 °C before conductively cooling on ascent (Proskurowski et al., 2006; Seyfried et al., 2015). Rates of H_2 production due to serpentinization are substantially lower at lower temperatures, but are not entirely halted (Mayhew et al., 2013; McCollom et al., 2016).

In contrast to H_2 , temperatures >350 °C appear to be necessary to overcome the kinetic inhibition to CH_4 formation (McCollom and Seewald, 2007). The isotopic signatures of CH_4 in LCHF fluids indicate that it formed abiotically at temperatures higher than those present in the modern system (Wang et al., 2018). Therefore, CH_4 likely formed early in the system when temperatures were hotter, was stored over millennia, and was stripped from the rocks into modern fluids (McDermott et al., 2015; Wang et al., 2018).

A model of extensive lower-temperature fluid flow across the top of the massif is also supported by alteration mineralogies, $\delta^{18}O$ signatures, and rare earth element abundances in the Expedition 357 cores, which indicate that localized fluid pathways across the southern wall are interconnected to form independent 100-m- to 1-km-sized cells (Roumejon et al., 2018). Relict olivine is present in central and eastern boreholes (M0068, M0072, M0076; Früh-Green et al., 2017, 2018), where H_2 is most abundant (Tables S1 and S2), indicating early serpentinization did not go to completion and could be ongoing. The high permeability in this region results from microfractures and the mesh texture of serpentinized peridotite (Roumejon et al., 2018), common features in ultramafic rocks due to the volume expansion and uptake

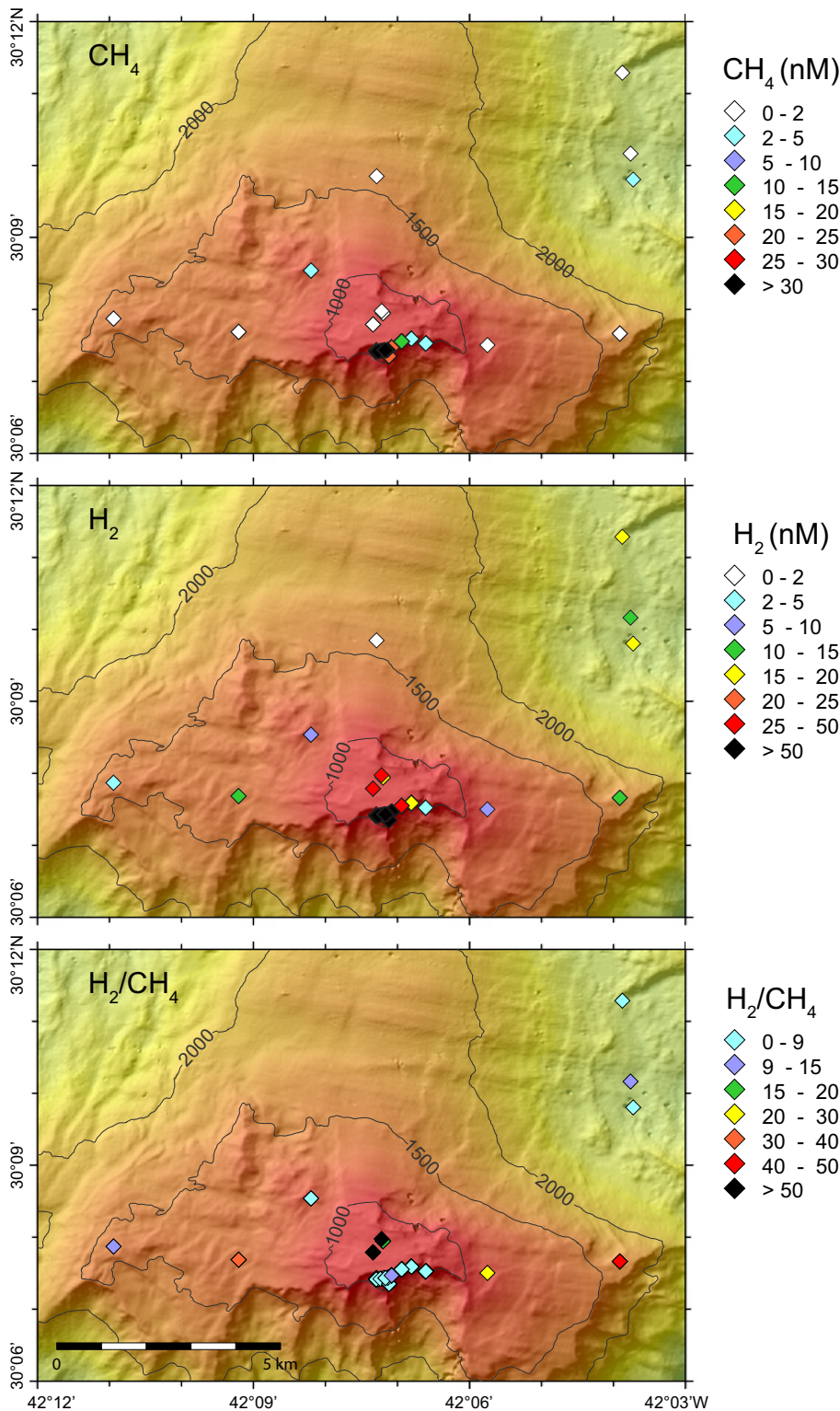


Figure 3. Distribution of CH_4 (nM), H_2 (nM), and H_2/CH_4 (mol/mol) ratios across the Atlantis Massif. Highest H_2 and CH_4 concentrations and lowest H_2/CH_4 ratios are above the Lost City Hydrothermal Field (LCHF). Lines are 500 m depth contours; color scale is the same as in Figure 1A.

of water during serpentinization (MacDonald and Fyfe, 1985).

Implications for the Early Evolution of Life

Serpentinization-fueled hydrothermal systems have been proposed as potential locations for the

origin and evolution of the first biochemical pathways due to the thermodynamic drive supplied by H_2 , the alkaline conditions that are favorable for prebiotic chemistry, and the redox and pH gradients that promote biochemical reactions (Martin and Russell, 2007; Sojo et al., 2016).

Proponents of a “small warm pond” for the origin of life emphasize the important roles of wet-dry cycles to promote polymerization (Frenkel-Pinter et al., 2020) and of clay minerals for forming and replicating biopolymers with specific sequences (Yu et al., 2013). Dispersed, low-flow circulation across the Atlantis Massif may create similar micro-environments of fluctuating water availability as water is consumed during serpentinization, followed by stages of higher water activity (Nascimento Vieira et al., 2020; Roumejon et al., 2018). Furthermore, serpentinization leads to the formation of serpentine and smectite clays (e.g., saponite) (MacDonald and Fyfe, 1985), which are similar to the montmorillonite clays most commonly invoked in origin-of-life hypotheses (Yu et al., 2013). Therefore, the widespread, localized flux of low-temperature, H_2 -bearing fluids through micro-environments containing clay minerals and fluctuating water availability may have been more conducive to the synthesis of the first biomolecules than the channelized flow of higher-temperature fluids through the central field.

Problematically, ancient serpentinization systems may have been starved for sulfur. Metal-sulfide minerals are thought to have been central to the origin of biochemical pathways as the catalytic templates of the first enzymes (Camprubi et al., 2017; Martin and Russell, 2007; Weiss et al., 2017). Sulfur in modern ultramafic rocks is largely derived from seawater sulfate (Alt et al., 2013), and ancient prebiotic oceans had <1% of the inorganic sulfur content of modern oceans (Crowe et al., 2014). The peridotite-dominated southern wall, where nonchannelized fluid flow is dominant, contains ~30% gabbro intrusions (Boschi et al., 2006; Früh-Green et al., 2018; Karson et al., 2006; Roumejon et al., 2018), and there is evidence that the sulfur in these mafic rocks is transferred into the peridotites (Liebmann et al., 2018). Therefore, the nonchannelized fluids may have entrained sufficient quantities of sulfur to make metal-sulfide catalysts available for primitive biochemical reactions in the serpentinite subsurface.

CONCLUSION

We documented the export of reducing, H_2 -rich fluids over a large geographical area across the Atlantis Massif, likely due to continuing serpentinization of the high-permeability, peridotite-dominated southern wall. The elevated H_2/CH_4 ratios of these widely distributed fluids indicate that they have a localized source distinct from the central LCHF. The geological features leading to this type of extensive circulation are common in oceanic core complexes and therefore possibly widespread in the world’s ocean. On ancient Earth, similar circulation of low-temperature, H_2 -rich fluids through micro-environments within the ocean crust could have

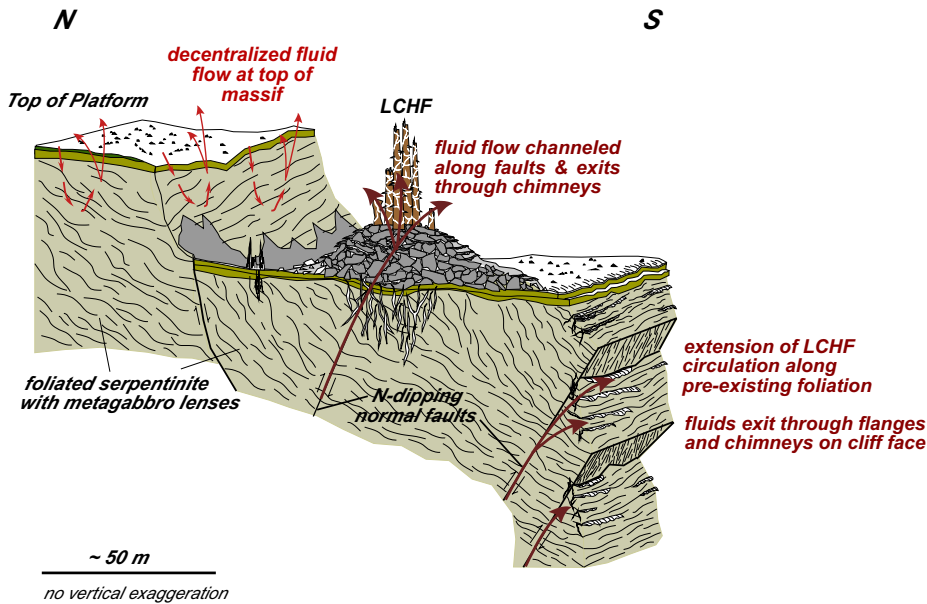


Figure 4. Fluid pathways at the the Atlantis Massif. Steep normal faults channel fluid outflow that creates the Lost City Hydrothermal Field (LCHF). Extensive, independent network of fluid flow also occurs away from the main circulation system. Figure is adapted from Kelley et al. (2005).

provided the fuel, sulfur, and fluctuating water availability necessary for the formation of early enzymes.

ACKNOWLEDGMENTS

We thank the captains and crews of the RRS *James Cook*, R/V *Atlantis*, the British Geological Survey's Remote Drill Two (RD2), Maurum's Meeresboden-Bohrgerät (MeBO), and ROV *Jason*, the scientific parties of both expeditions, Daniel Fornari for the use of the MISO camera, and John Baross for inspirational conversations. Funding was provided by National Science Foundation awards OCE-1536702, OCE-1536405, and OCE-1535962, the National Aeronautics and Space Administration (NASA) Astrobiology Institute "Rock Powered Life" team (CAN 7), the U.S. Science Support Program of the International Ocean Discovery Program (IODP), European Consortium for Ocean Research Drilling (ECORD), the Deep Carbon Observatory, and Swiss National Science Foundation project 200021_163187 (to G. Früh-Green). This is Pacific Marine Environmental Laboratory (PMEL) contribution 5151. We thank editor Gerald Dickens and two anonymous reviewers for comments that improved the manuscript.

REFERENCES CITED

Alt, J.C., Schwarzenbach, E.M., Früh-Green, G.L., Shanks, W.C., Bernasconi, S.M., Garrido, C.J., Crispini, L., Gaggero, L., Padron-Navarta, J.A., and Marchesi, C., 2013, The role of serpentinites in cycling of carbon and sulfur: Seafloor serpentinization and subduction metamorphism: *Lithos*, v. 178, p. 40–54, <https://doi.org/10.1016/j.lithos.2012.12.006>.

Boschi, C., Früh-Green, G.L., Delacour, A., Karson, J.A., and Kelley, D.S., 2006, Mass transfer and fluid flow during detachment faulting and development of an oceanic core complex, Atlantis Massif (MAR 30°N): *Geochemistry Geophysics Geosystems*, v. 7, Q01004, <https://doi.org/10.1029/2005GC001074>.

Camprubi, E., Jordan, S.F., Vasiliadou, R., and Lane, N., 2017, Iron catalysis at the origin of

life: *IUBMB Life*, v. 69, p. 373–381, <https://doi.org/10.1002/iub.1632>.

Crowe, S.A., Paris, G., Katsev, S., Jones, C., Kim, S.T., Zerkle, A.L., Nomosatryo, S., Fowle, D.A., Adkins, J.F., Sessions, A.L., Farquhar, J., and Canfield, D.E., 2014, Sulfate was a trace constituent of Archean seawater: *Science*, v. 346, p. 735–739, <https://doi.org/10.1126/science.1258966>.

Denny, A.R., Kelley, D.S., and Früh-Green, G.L., 2016, Geologic evolution of the Lost City Hydrothermal Field: *Geochemistry Geophysics Geosystems*, v. 17, p. 375–394, <https://doi.org/10.1002/2015GC005869>.

Fisher, A.T., 2004, Rates of flow and patterns of fluid circulation, in Elderfield, E.E.D., et al., eds., *Hydrogeology of the Oceanic Lithosphere*: Cambridge, UK, Cambridge University Press, p. 339–377.

Frenkel-Pinter, M., Samanta, M., Ashkenasy, G., and Leman, L.J., 2020, Prebiotic peptides: Molecular hubs in the origin of life: *Chemical Reviews*, v. 120, p. 4707–4765, <https://doi.org/10.1021/acs.chemrev.9b00664>.

Früh-Green, G.L., et al., 2017, Eastern sites, in Früh-Green, G.L., et al., eds., *Proceedings of the International Ocean Discovery Program Volume 357*: College Station, Texas, International Ocean Discovery Program, <https://doi.org/10.14379/iodp.proc.357.103.2017>.

Früh-Green, G.L., et al., 2018, Magmatism, serpentinization and life: Insights through drilling the Atlantis Massif (IODP Expedition 357): *Lithos*, v. 323, p. 137–155, <https://doi.org/10.1016/j.lithos.2018.09.012>.

Kadko, D.C., Rosenberg, N.D., Lupton, J.E., Collier, R.W., and Lilley, M.D., 1990, Chemical-reaction rates and entrainment within the Endeavor Ridge hydrothermal plume: *Earth and Planetary Science Letters*, v. 99, p. 315–335, [https://doi.org/10.1016/0012-821X\(90\)90137-M](https://doi.org/10.1016/0012-821X(90)90137-M).

Karson, J.A., Früh-Green, G.L., Kelley, D.S., Williams, E.A., Yoerger, D.R., and Jakuba, M., 2006, Detachment shear zone of the Atlantis Massif core complex, Mid-Atlantic Ridge, 30°N: *Geochemistry Geophysics Geosystems*, v. 7, Q06016, <https://doi.org/10.1029/2005GC001109>.

Kelley, D.S., et al., 2005, A serpentinite-hosted ecosystem: The Lost City Hydrothermal Field: *Science*, v. 307, p. 1428–1434, <https://doi.org/10.1126/science.1102556>.

Lang, S.Q., Früh-Green, G.L., Bernasconi, S.M., Lilley, M.D., Proskurowski, G., Mehay, S., and Butterfield, D.A., 2012, Microbial utilization of abiogenic carbon and hydrogen in a serpentinite-hosted system: *Geochimica et Cosmochimica Acta*, v. 92, p. 82–99, <https://doi.org/10.1016/j.gca.2012.06.006>.

Larson, B.I., Lang, S.Q., Lilley, M.D., Olson, E.J., Lupton, J.E., Nakamura, K., and Buck, N.J., 2015, Stealth export of hydrogen and methane from a low temperature serpentinization system: Deep-Sea Research: Part II, Topical Studies in Oceanography, v. 121, p. 233–245, <https://doi.org/10.1016/j.dsr2.2015.05.007>.

Liebmann, J., Schwarzenbach, E.M., Früh-Green, G.L., Boschi, C., Roumejon, S., Strauss, H., Wiechert, U., and John, T., 2018, Tracking water-rock interaction at the Atlantis Massif (MAR, 30°N) using sulfur geochemistry: *Geochemistry Geophysics Geosystems*, v. 19, p. 4561–4583, <https://doi.org/10.1029/2018GC007813>.

MacDonald, A.H., and Fyfe, W.S., 1985, Rates of serpentinization in seafloor environments: *Tectonophysics*, v. 116, p. 123–135, [https://doi.org/10.1016/0040-1951\(85\)90225-2](https://doi.org/10.1016/0040-1951(85)90225-2).

Martin, W., and Russell, M.J., 2003, On the origins of cells: A hypothesis for the evolutionary transitions from abiotic geochemistry to chemoautotrophic prokaryotes, and from prokaryotes to nucleated cells: *Philosophical Transactions of the Royal Society [London]: Series B, Biological Sciences*, v. 358, p. 59–85, <https://doi.org/10.1098/rstb.2002.1183>.

Martin, W., and Russell, M.J., 2007, On the origin of biochemistry at an alkaline hydrothermal vent: *Philosophical Transactions of the Royal Society [London]: Series B, Biological Sciences*, v. 362, p. 1887–1926, <https://doi.org/10.1098/rstb.2006.1881>.

Mayhew, L.E., Ellison, E.T., McCollom, T.M., Trainor, T.P., and Templeton, A.S., 2013, Hydrogen generation from low-temperature water-rock reactions: *Nature Geoscience*, v. 6, p. 478–484, <https://doi.org/10.1038/ngeo1825>.

McCaig, A.M., Cliff, R.A., Escartin, J., Fallick, A.E., and MacLeod, C.J., 2007, Oceanic detachment faults focus very large volumes of black smoker fluids: *Geology*, v. 35, p. 935–938, <https://doi.org/10.1130/G23657A.1>.

McCollom, T.M., and Seewald, J.S., 2007, Abiotic synthesis of organic compounds in deep-sea hydrothermal environments: *Chemical Reviews*, v. 107, p. 382–401, <https://doi.org/10.1021/cr0503660>.

McCollom, T.M., Klein, F., Robbins, M., Moskowitz, B., Berquo, T.S., Jons, N., Bach, W., and Templeton, A., 2016, Temperature trends for reaction rates, hydrogen generation, and partitioning of iron during experimental serpentinization of olivine: *Geochimica et Cosmochimica Acta*, v. 181, p. 175–200, <https://doi.org/10.1016/j.gca.2016.03.002>.

McDermott, J.M., Seewald, J.S., German, C.R., and Sylva, S.P., 2015, Pathways for abiotic organic synthesis at submarine hydrothermal fields: *Proceedings of the National Academy of Sciences of the United States of America*, v. 112, p. 7668–7672, <https://doi.org/10.1073/pnas.1506295112>.

Nascimento Vieira, A.D., Kleinermanns, K., Martin, W.F., and Preiner, M., 2020, The ambivalent role of water at the origins of life: *FEBS Letters*, v. 594, p. 2717–2733, <https://doi.org/10.1002/1873-3468.13815>.

- Proskurowski, G., Lilley, M.D., Kelley, D.S., and Olson, E.J., 2006, Low-temperature volatile production at the Lost City Hydrothermal Field, evidence from a hydrogen stable isotope geothermometer: *Chemical Geology*, v. 229, p. 331–343, <https://doi.org/10.1016/j.chemgeo.2005.11.005>.
- Proskurowski, G., Lilley, M.D., Seewald, J.S., Früh-Green, G.L., Olson, E.J., Lupton, J.E., Sylva, S.P., and Kelley, D.S., 2008, Abiogenic hydrocarbon production at Lost City Hydrothermal Field: *Science*, v. 319, p. 604–607, <https://doi.org/10.1126/science.1151194>.
- Roumejon, S., Früh-Green, G.L., Orcutt, B.N., and Party, I.E.S., 2018, Alteration heterogeneities in peridotites exhumed on the southern wall of the Atlantis Massif (IODP Expedition 357): *Journal of Petrology*, v. 59, p. 1329–1358, <https://doi.org/10.1093/ptrology/egy065>.
- Seyfried, W.E., Pester, N.J., Tutolo, B.M., and Ding, K., 2015, The Lost City hydrothermal system: Constraints imposed by vent fluid chemistry and reaction path models on seafloor heat and mass transfer processes: *Geochimica et Cosmochimica Acta*, v. 163, p. 59–79, <https://doi.org/10.1016/j.gca.2015.04.040>.
- Sojo, V., Herschy, B., Whicher, A., Camprubi, E., and Lane, N., 2016, The origin of life in alkaline hydrothermal vents: *Astrobiology*, v. 16, p. 181–197, <https://doi.org/10.1089/ast.2015.1406>.
- Titarenko, S.S., and McCaig, A.M., 2016, Modelling the Lost City Hydrothermal Field: Influence of topography and permeability structure: *Geofluids*, v. 16, p. 314–328, <https://doi.org/10.1111/gfl.12151>.
- Von Damm, K.L., and Lilley, M.D., 2004, Diffuse flow hydrothermal fluids from 9°50'N East Pacific Rise: Origin, evolution and biogeochemical controls, *in* Wilcock, W.S.D., et al., eds., *The Seafloor Biosphere at Mid-Ocean Ridges: American Geophysical Union Geophysical Monograph 144*, p. 245–268, <https://doi.org/10.1029/144GM16>.
- Wang, D.T., Reeves, E.P., McDermott, J.M., Seewald, J.S., and Ono, S., 2018, Clumped isotopologue constraints on the origin of methane at seafloor hot springs: *Geochimica et Cosmochimica Acta*, v. 223, p. 141–158, <https://doi.org/10.1016/j.gca.2017.11.030>.
- Wankel, S.D., Germanovich, L.N., Lilley, M.D., Genc, G., DiPerna, C.J., Bradley, A.S., Olson, E.J., and Girguis, P.R., 2011, Influence of subsurface biosphere on geochemical fluxes from diffuse hydrothermal fluids: *Nature Geoscience*, v. 4, p. 461–468, <https://doi.org/10.1038/ngeo1183>.
- Weiss, M.C., Sousa, F.L., Mrnjavac, N., Neukirchen, S., Roettger, M., Nelson-Sathi, S., and Martin, W.F., 2017, The physiology and habitat of the last universal common ancestor: *Nature Microbiology*, v. 1, <https://doi.org/10.1038/nmicrobiol.2016.116>.
- Yu, W.H., Li, N., Tong, D.S., Zhou, C.H., Lin, C.X., and Xu, C.Y., 2013, Adsorption of proteins and nucleic acids on clay minerals and their interactions: A review: *Applied Clay Science*, v. 80–81, p. 443–452, <https://doi.org/10.1016/j.clay.2013.06.003>.

Printed in USA